An Investigation of Heat Transfer Characteristics of Swirling Flow in a 180° Circular Section Bend with Uniform Heat Flux

Tae-Hyun Chang*

Division of Mechanical and Automation Engineering, Kyungnam University, 440 Wolyoung Dong, Masan Kyungnam, Korea

An experiment was performed to obtain the local heat transfer coefficient and Nusselt number in a circular duct with a 180° bend for $Re=6\times10^4$, 8×10^4 and 1×10^5 under swirling flow and non-swirling flow conditions. The test tube with a circular section was made from stainless steel having a curvature ration of 9.4. Current heat flux of 5.11 kW/m^2 was applied to the test tube by electrical power and the swirling motion of air was produced by a tangential inlet to the pipe axis at 180°. Measurements of local wall temperatures and the bulk mean temperatures of air were made at four circumferential positions at 16 stations. The wall temperatures showed a reduced distribution curve at the bend for the non-swirling flow, but this effect did not appear for the swirling flow. The Nusselt number distributions for the swirling flow, which was calculated from the measured wall and the bulk temperatures, were higher than that of the non-swirling flow. The average Nusselt number of the swirling flow increased by about 90-100%, compared to that of the non-swirling flow. The Nu/Nu_{DB} values at the 90° station for non-swirling flow and swirling flow were approximately 2.5 and 4.8 at $Re=6\times10^4$ respectively. The values agree well with Said's results for non-swirling flow.

Key Words : Swirling Flow, Non Swirling Flow, Swirl Chamber, Swirl Generator, Wall Temperature, Bulk Temperature, Uninform Heating

Nomenclature

A : Cross-sectional area of the test tube.
C_p : Specific heat at constant pressure.
d : Inner diameter of swirl chamber.
D : Inner diameter of the test tube.
h : heat transfer coefficient.
h_{ij} : Local convection heat transfer coefficient.
L : Distance along the swirl chamber.
L/D : Intensity of swirl flow.
$\dot{m}$: Mass flow rate
Nu : Nusselt number.
Nu_{DB} : Nusselt number for fully developed flow
q : Heat flux.
r : Inner radius of the bend.
R : Bend mean radius.
Rc : Curvature Radius.
Re : Reynolds number.
T : Temperature of fluid.
T_b : Bulk temperature.
T_w : Wall temperature.
x : Axial length.
x/D : Non-dimensional length.
y : Radial distance from a tube wall.
θ : Angle of U-bend.

* **E-mail** : changtae@kyungnam.ac.kr
TEL : +82-55-249-2613; **FAX** : +82-55-249-2617
Division of Mechanical and Automation Engineering, Kyungnam University, 440 Wolyoung Dong, Masan Kyungnam, Korea. (Manuscript **Received** May 20, 2002; **Revised** August 19, 2003)

1. Introduction

The flow in a U-bend, which is more complicated than that in a straight tube, has been a subject of research. In particular, convection heat transfer in a U-bend, which has a curvature in the flow direction, has been applied to the design of heat exchangers and condensers in a power sta-

tion, the design of turbine blades cooling, and other such designs.

The fluid flow pressure through a U-bend is increased when the flow is moved from the center of the bend to the outer wall direction and decreased from the center to the inner wall. It is in the vertical section of the main stream flow that the fluid pressure loss is forced towards the center of the bend and a high speed fluid near the axis is pushed outwards. Here, a secondary flow, which overlaps with the axial velocity, is constituted. In other words, a strong section flow occurs from the inner movement of a flow field around the bend.

A secondary flow was found initially in a channel flow by Thomson (1876). After that, a fully developed flow of the bend was measured by a pitot-tube, a hot-wire anemometry flow meter, etc. Recently, by making good use of LDA, much of the flow pattern data has been provided. Also, one of important study of turbulent swirling flow was carried by Chang et al(2001) using particle image velocimetry techniques.

Ito (1960) presented the importance of pressure loss in a bend, and Yianneskis et al.(1982) measured the characteristics of laminar and turbulent flows through a right-bend by the Laser-Doppler method so that a secondary flow formed inside a bend could be found. Johnson (1988) has investigated the fluid flow of the U-bend that had a rectangular cross-sectional shape by using the numerical analysis method, while Chang et al. (1988) discussed the fluid flow and heat transfer in a rectangular bend. Such research is related to fluid flow in a specific geometrically shaped tube. The characteristics of heat transfer depend on the state of fluid flow and show different phenomena by various methods of heating and measurement.

With the characteristics of heat transfer in a bent tube, Metha et al.(1981) presented the heat transfer coefficient of a laminar flow. It is notable that the generation of heat was implemented through an electrode, which was installed directly to the U-bend, by using DC voltage, they, however, presented the characteristics of the heat transfer coefficient after measuring the wall temperature of the upper and the lower stream areas excluding the bend. Iacovide et al.(1987) created a uniform heat stream by winding a heating coil over a bend made of brass cast, and the ratio between the bend radius and the tube diameter was 3.375. They measured the optimal bulk temperature, investigated the characteristics of Nusselt number, and found that the maximum of the value was located in the middle of the bend. Between the wall temperature and the bulk temperature, which is influenced by the heat transfer coefficient, it can be seen that Metha et al. had calculated the former and Iacovide et al. the latter. While both Metha et al. and Iacovide et al. presented the characteristics of the heat transfer, neither group commented on the improvement of the heat transfer. In the design processes of heat exchangers, emphasis has been placed on utilizing energy effectively. Therefore, it is important to present how to improve the heat transfer coefficient. To date, it has been used to improve the heat transfer coefficient, make good use of an artificial illumination, and increase the area of heat transfer by utilizing a helical surface, wire coil, fin etc.

A method different from the enlargement of the contact area is to increase the intensity of the turbulent flow by adding swirling flow. Talbot (1954) derived the equation for laminar swirling flow in a straight tube and studied the nullification phenomenon of swirling flow. Chang et al.(1989) had studied the friction coefficient and the velocity component of swirling flow and, through the flow visualization process, presented the swirl angle of swirling flow. Theoretically, the stream line of tangential flow with swirl is longer than that of non-swirling so that fluid particles, which are located near the heated tube wall, can deliver more energy to the fluid flow. Therefore it is possible to improve the heat transfer coefficient.

For this research, a U-bend, which was fabricated by high frequency induction bending and whose material itself had been utilized as a electrical resistance, was directly heated by DC and performed heat transfer experiments. At the entrance of the tube apparatus, the swirl generator (⑱, ⑲) had been installed and could generate the swirling flow. After the wall and the air temperatures were directly measured according to

the variable momentum value of non-swirling and swirling flow, the temperature distribution relationship from the effect of the bend tube and swirling flow, was identified. Then Nusselt number was defined and the characteristics of the heat transfer were also investigated.

2. Experimentation

2.1 Experimental apparatus

Figure 1 shows the schematic diagram of the experimental apparatus, and Fig. 2 shows a photograph of the test tube.

The test tube whose material was stainless steel 304 and ID 54.5 mm (thickness 3 mm) had been fabricated to a bend radius of R=255 mm by higher frequency induction bending. Therefore, the curvature ratio ($R_c=R/r$) of the U-bend was 9.4. The test tube consisted of an upstream, the bend and the downstream tube. The reference point was located at the entrance of the bend. The specifications of the test tube are shown in Table 1.

For the non-swirling flow, a straight tube, whose flange could attach to a swirl chamber was attached to the bend entrance to create a fully developed flow.

In order to generate a swirling flow, a flange for the swirl chamber was installed in this research. The structure of the swirl chamber is

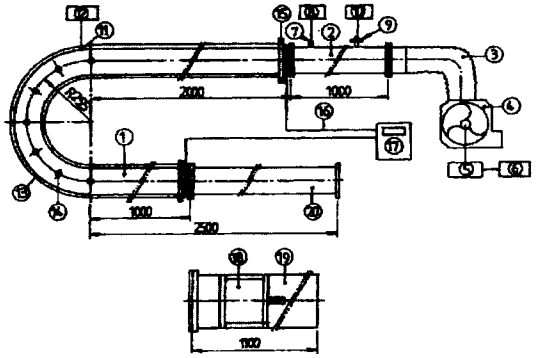

1. Test tube (φ54.5)
2. Steel tube
3. Flexible hose
4. Turbo fan
5. Motor (220V · 10HP)
6. R.P.M. controller
7. Pitot tube
8. Electronic Manometer
9. Multi pitot tube
10. Inclied manometer
11. Thermocouple (K type)
12. Thermometer (HR2500)
13. Insulation
14. Measureing hole (φ3)
15. Copper connector
16. Lead wire (φ30)
17. Voltage regulator (20 kw)
18. Swirl generator
19. Swirl chamber
20. Stainless tube (φ54.5)

Fig. 1 Schematic diagram of the experimental apparatus

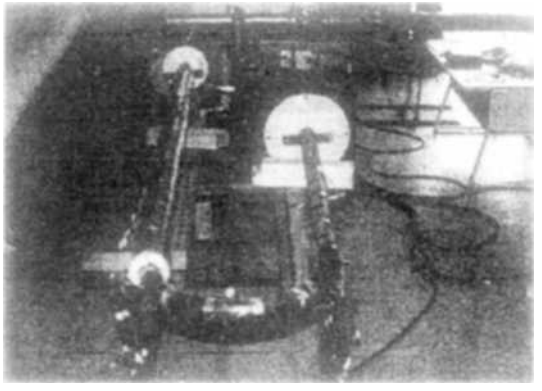

Fig. 2 Photograph of the test tube

Table 1 Specifications of the test tube

Material			SUS 304
Tube diameter	Outer	mm	60.5
	Inner (D)	mm	54.5
Upstream Straight section		mm	2500
Bend mean radius (R)		mm	255
Curvature ratio (R_c)			9.4
Heat flux		kw/m^2	5.11

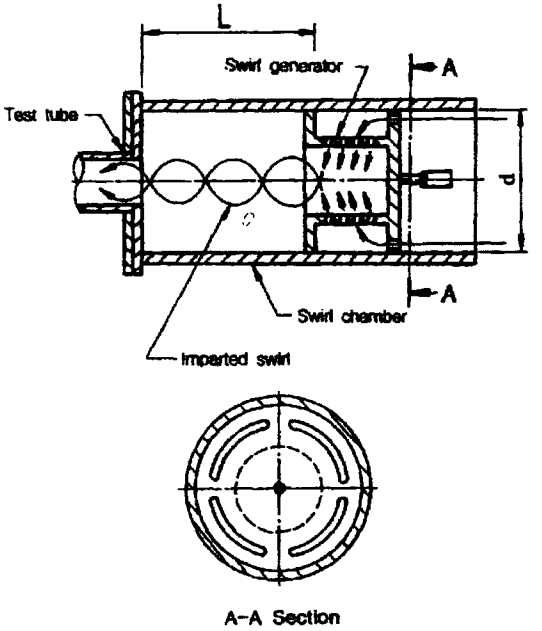

Fig. 3 Schematic diagram of inlet section

shown in Fig. 3. The swirl generator, which was made of acryl, was drilled with $28 \times \phi 3.2$ mm holes in the cylinder wall, which was 45° equally spaced on the circumference of a circle, as shown in Fig. 4.

In the swirl generator of the swirl chamber, air is introduced through slot holes, which are shown in section A-A, then a swirl flow is generated and flowed into the test tube. At that moment, the swirl balance was maintained by the back plate of the swirl generator. The intensity of the swirl flow was determined by the ratio (L/D), where L is the length of the swirl chamber and D is the inner diameter of the test tube.

To keep the test tube heated uniformly, 4 pieces of 30 mm copper cable were connected from the voltage regulator to the connection pin of the test tube and 5.11 kW/m^2 of power (current 650A, voltage 5.4V) was directly supplied to it. To insulate the test tube, insulation was wrapped in a blanket of 30 mm of fiberglass and overlapped with vinyl tape.

The wall temperature was measured at 3 stations in the upstream of the test tube, 7 stations in the U-bend, and 6 stations in the downstream by K-type thermocouples, which were connected to a Hybrid recorder (HR2500). The thermocouples had been calibrated and fixed to the test tube wall by heat resistance tape so that they could be prevented from separating from the tube.

To obtain the bulk temperatures of the flow at the same station where the wall temperature was measured, thermocouples were installed at the top and outside guide holes, which were drilled with $\phi 3$ mm holes on the test tube wall, fitted with size $\phi 3$ mm and length 40 mm tubes, and fixed with epoxy adhesive (devcon epoxy), as shown in Fig. 5. The air temperatures were measured at the 7 points in each station, as shown in Table 3. The bulk temperature was calculated from the equation 6 and 7.

Table 2 Measurement stations of temperature

Test tube	Number of test stations	Nondimensional distance (x/D)
Upstream	1	−10
	2	−6
	3	−2
Bend	4	0°
	5	30°
	6	60°
	7	90°
	8	120°
	9	150°
	10	180°
Downstream	11	1
	12	3
	13	6
	14	10
	15	16
	16	24

Table 3 Measurement positions of the bulk temperature

Measuring positions	0~0.5~1.5~3.5~6.5~11.5~18.5~27.25 (wall) (center)						
Interval [mm]	0.5	1	2	3	5	7	8.75

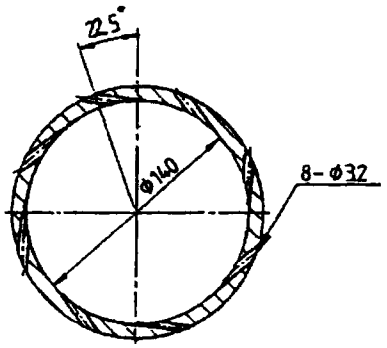

Fig. 4 Cross-section of the swirl generator

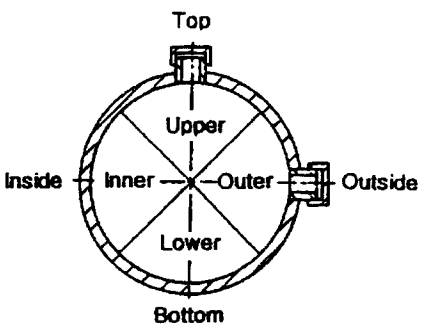

Fig. 5 Cross-section of the test tube

2.2 Experimental method

A multi-pitot tube (TORBAR 301) was installed at the end of the test tube. With the tube, the calibration curve was obtained. The required Reynolds number was obtained by adjusting the fan operation so that the average velocity on the Reynolds number might be converted to the measured total and static pressures.

AC power (650A×5.4V=3.51 kW) was supplied to the test tube to obtain the uniformly heated fluid. The test was carried out 12 times for the non-swirling flow, the strong swirling ($L/D=0$), the medium swirling ($L/D=7$), and the weak swirling ($L/D=14$) flow. The Reynolds numbers of the test tube entrance were 6×10^4, 8×10^4 and 1×10^5.

To maintain uniformly the heated fluid, first, the Reynolds number was set up by adjusting the fan operation and second, the fluid was heated by the AC current, which was flowed from the voltage regulator to the test tube. After the fluid in the test tube had been heated for 30 minutes, it was uniformly heated. After that, the data for 64 points were measured and recorded simultaneously for the bulk and the wall temperature at the startup, the middle, and the final experimentation. These data were calculated as the mean value and deleted over a 3% standard deviation.

2.3 Calculation equation

Using the current and voltage data, which were directly supplied to the fluid through the voltage regulator, the heated fluid can be calculated as follows

$$Q_{conv}=(I)\times(V) \tag{1}$$

In the heat balance, the percent of error is as follows:

$$\%\text{error}=\frac{Q_{input}-Q_{output}}{Q_{input}}\times100 \tag{2}$$

The heat supplied to the test tube is as follows:

$$Q_{input}=I\cdot V-Q_{loss} \tag{3}$$

The heat lost in the test tube is as follows:

$$Q_{output}=\dot{m}\,[(T_b)_{i+1}-(T_b)_i] \tag{4}$$

In the test tube, the local flow temperature was directly measured by the thermocouples, and then compared with the calculation of the following equation.

The average wall temperature of a section is as follows:

$$(T_w)_i=\frac{1}{4}\sum_{j=1}^{4}(T_w)_{ij} \tag{5}$$

The bulk temperatures was measured at 7 points in each section, which divided the tube cross-sectionally into 4 sections. Therefore,

$$(T_b)_{ij}=\frac{1}{7A}\sum_{j=1}^{7}[(T_b)_{ij}]\,dA \tag{6}$$

$$(T_b)_i=\frac{1}{4}\sum_{i=1}^{4}(T_b)_{ij} \tag{7}$$

"A" denotes the cross-section of the test tube.

After the wall and the bulk temperatures were obtained, the local and the average local heat transfer coefficient can be derived from the following equation.

$$q_{ij}=C_p[(T_b)_{i+1,j}-(T_b)_{ij}] \tag{8}$$

$$h_{ij}=\frac{q_{ij}}{[(T_w)_{ij}-(T_b)_{ij}]} \tag{9}$$

$$\bar{h}_i=\frac{1}{4}\sum_{j=1}^{4}(h_{ij}) \tag{10}$$

From the convection heat transfer coefficient h_{ij}, the Nusselt number was obtained.

$$Nu=\frac{h\cdot D}{k} \tag{11}$$

3. Results and Discussions

3.1 The wall temperature

When a circular tube is internally heated and wrapped with an insulator, the wall and the bulk temperature will slightly affect the average convection heat transfer coefficient of the fluid. Such temperature distribution will depend upon the characteristics of a fluid flow, so this research was based on the model that Miller et al.(1980) had studied regarding the fluid flow of the U-bend.

Figure 6 shows the wall temperature profile of the non-swirl flow on the top, bottom, inside, and outside positions at the upstream, bend, and

downstream of the test tube for $Re=1\times10^5$. The temperatures for 4 positions at the upstream were almost the same, but there were 15℃ differences between the inside and outside positions at the bend entrance.

The temperature of the inside position was the highest at $\theta=30°$, the lowest at $\theta=90°$, and, after $\theta=90°$, gradually increased. The wall temperatures at the top and bottom positions were almost the same throughout the bend. Because the phenomenon of a fluid flow near the tube wall is keenly related to the temperature of the tube wall, these results show that the fluid flow partially accelerated from the tube entrance.

Figure 7 shows the wall temperature profiles along the test tube with the swirl intensity L/D= 14 for $Re=1\times10^5$. There were temperature differences, between the inside and outside positions, similar to the non-swirl flow, that started from the bend entrance but continually increased unlike the non-swirl flow. If only considering the swirl flow, the wall temperature profile is almost similar to that of the straight tube. Thus, the swirl flow is hardly affected by the geometrical shape of the bend and has heat transfer characteristics that are similar to those of the straight tube flow.

The temperatures for the 4 downstream positions of the bend are almost steady near 24D for the non-swirl flow and 6D for the swirl flow, meaning that in developing a turbulent flow in the downstream of the bend, the swirl flow can be done earlier than the non-swirl flow, as it were it can minimize the effect of the bend by the swirl flow.

Figure 8 shows the average wall temperature profiles along the test tube with the non-swirl flow for $Re=6\times10^4$, 8×10^4 and 1×10^5. The wall temperatures increase in the tube entrance, decreased in the bend, minimized near $\theta=90°$, and continuously increased in the downstream without regard to the Re. Here, the wall temperatures are reduced when the Reynolds number is increased due to an increase in the mass flow rate.

Figure 9, which is the average wall temperature profiles along the test tube with swirl of L/D= 7, shows a linear increase in the upstream and downstream bend and slightly high and nonlinear in the bend. When the temperature is compared with Fig. 8, it is an overall temperature drop and a peculiar temperature distribution curve. That is, the swirl flow seems to minimize the effects of the U-bend tube. Meanwhile, it

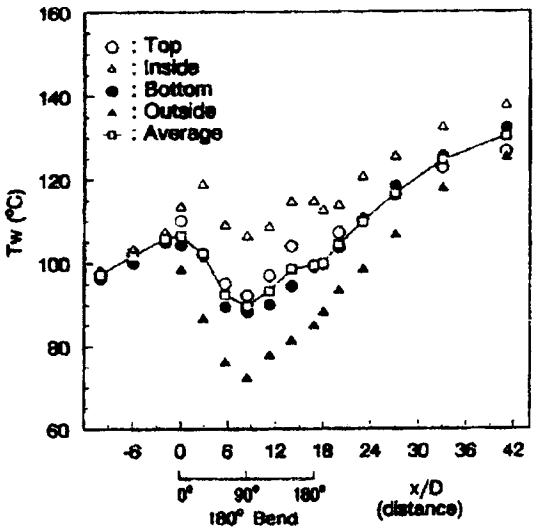

Fig. 6 Wall temperature profiles along the test tube with non-swirl form $Re=1\times10^5$

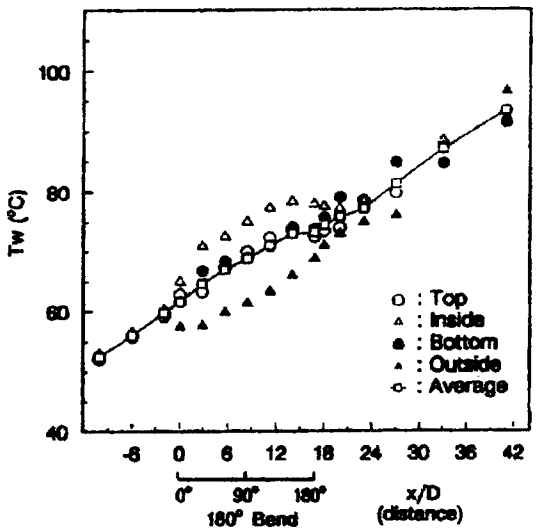

Fig. 7 Wall temperature profiles along the test tube with swirl of L/D=14 for $Re=1\times10^5$

affects the heat transfer coefficient.

Figure 10 shows the distribution of the temperature profiles between the inside and the outside positions along the U-bend with non-swirl flow for $Re=6\times10^4$, 8×10^4, and 1×10^5. The temperature differences between the inside and the outside positions occurred at the bend entrance and reached a maximum at 90°. At first the temperature at the outside position decreases and then increase, but at the inside, it temporarily increased from the bend entrance, and then, from $\theta=30°$, decreased and increased.

Figure 11 shows the distribution of the wall temperature profiles between the inside and the outside positions along the U-bend with swirl of L/D=7 for each Reynolds number. The temperature differences showed at the bend entrance

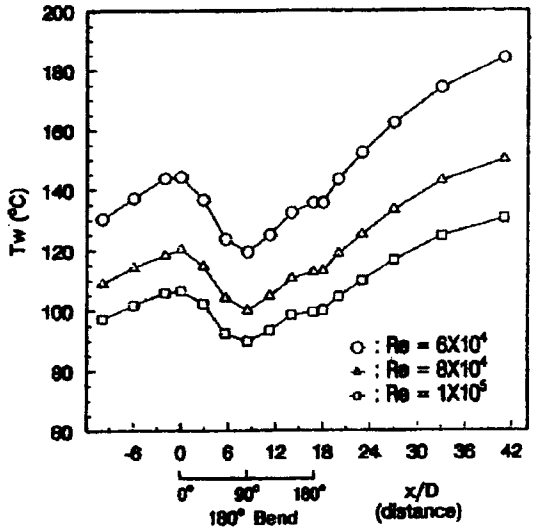

Fig. 8 Average wall temperature profiles along the test tube with non-swirl

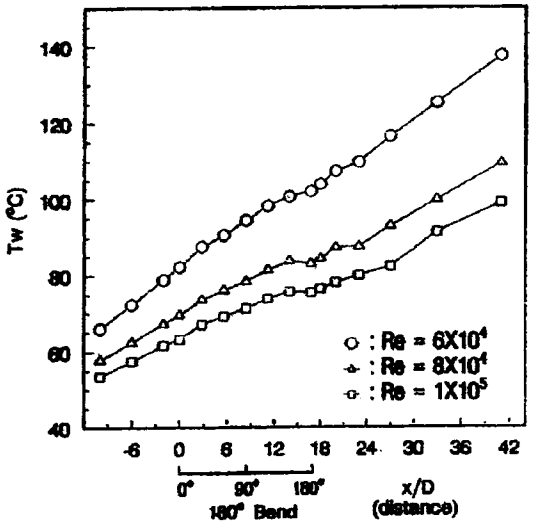

Fig. 9 Average wall temperature profiles along the test tube with of L/D=7

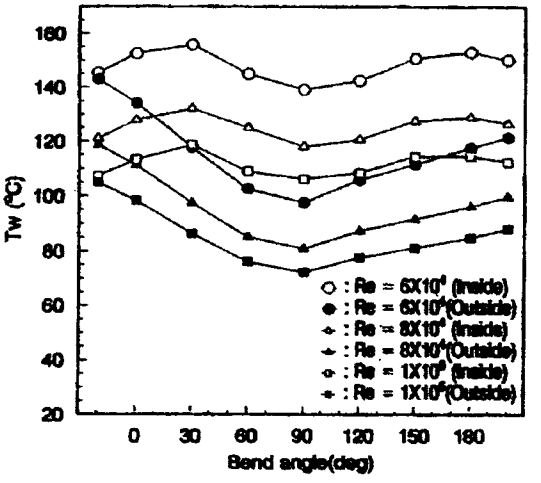

Fig. 10 Comparison of wall temperature profiles between inside and outside along 180° bend for non-swirl with respect to Re

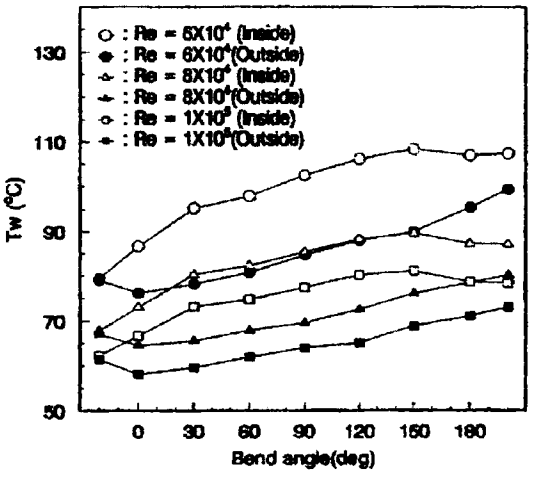

Fig. 11 Comparison of wall temperature profiles between inside and outside along 180° bend for swirl of L/D=7 with respect to Re

and increased between $\theta=30°$ and $\theta=150°$. The temperature differences between the inside and the outside of the non-swirl flow were bigger than that in the swirl flow. In general, the temperature distribution of the non-swirl flow was higher than that of the swirl. It arises from that in the bend tube the swirl flow is more accelerated than the non-swirl and furthermore is more activated in the generation of the secondary flow the swirl.

3.2 The bulk temperature

Figure 12 shows the results of the bulk temperatures measured at the upper, lower, inner, and outer positions of the tube, which were divided at the tubes cross-section where the wall temperature was measured.

For non-swirl flow, the bulk temperatures over the overall test tube are comparatively distributed in a big gap. Even though the bulk temperature between the upper and lower positions was little, the temperature gap between the inner and the outer positions was very large. The minimum difference was accomplished at $\theta=90°$, and increased again. Therefore, there is a possibility of maximum heat transfer at a $\theta=90°$ position of the bend.

The bulk temperature of an intensive swirl flow, which was measured at $Re=1\times10^5$, shows quite a different result from the non-swirl flow as shown in Fig. 13. The temperatures of all positions were uniformly distributed and increased linearly. Meaning that, due to an intensive swirl flow, there was no partial acceleration so that nearly constant temperature distributions

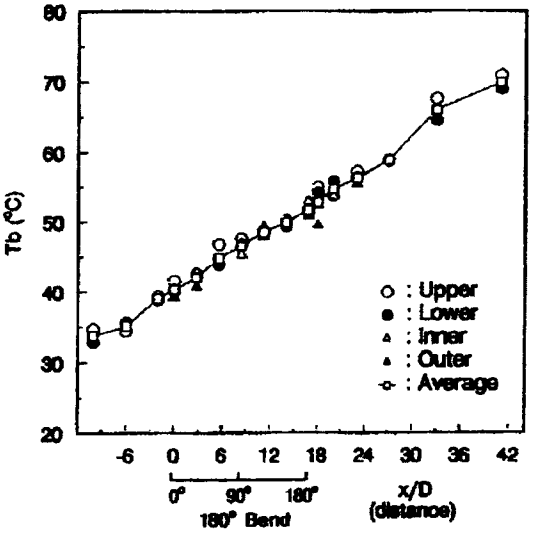

Fig. 13 Bulk temperature profiles along the test tube with swirl at L/D=0 for $Re=1\times10^5$

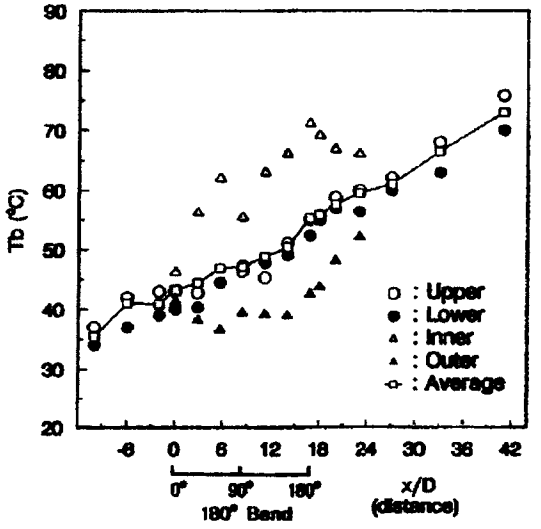

Fig. 12 Bulk temperature profiles along the test tube with non-swirl for $Re=1\times10^5$

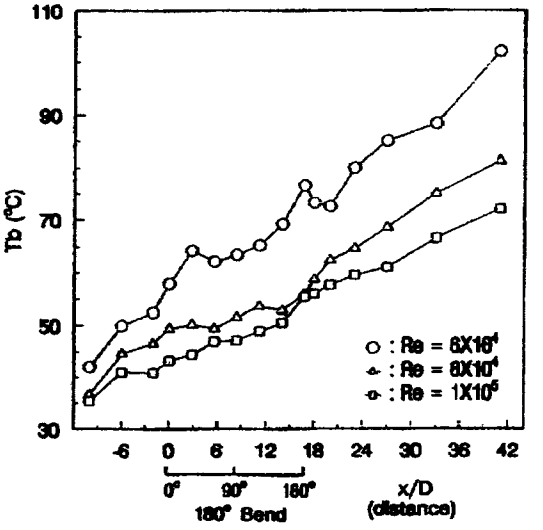

Fig. 14 Average bulk temperature profiles along the test tube with non-swirl

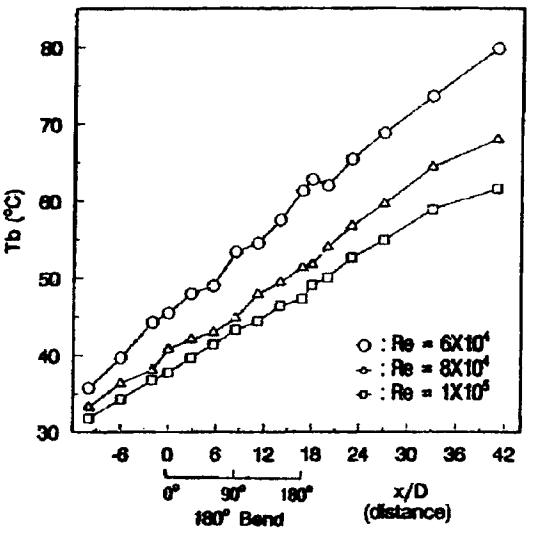

Fig. 15 Average bulk temperature profiles along the test tube with swirl at L/D=7

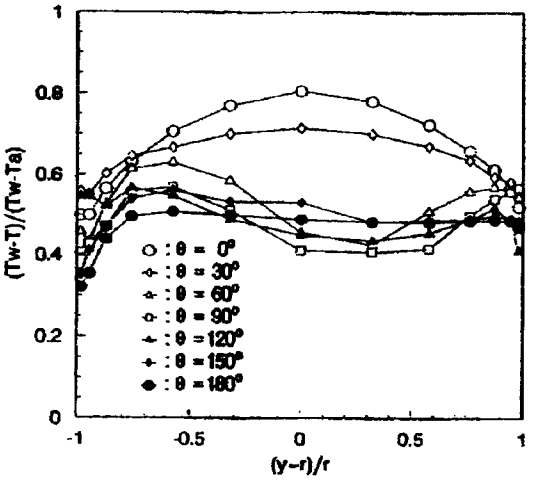

Fig. 16 Comparisons of (Tw−T)/(Tw−Ta) with variation from top to bottom for non swirl at Re=6×10⁴

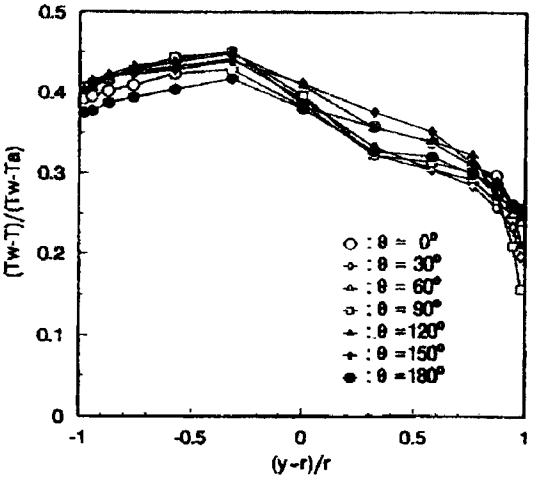

Fig. 17 Comparisons of (Tw−T)/(Tw−Ta) with variation from top to bottom for wirl L/D=0 at Re=6×10⁴

are shown throughout the length of the overall test tube. Figure 14 shows the average bulk temperature profiles along the test tube with non swirl flow, and Fig. 15 shows for each Reynolds number of the swirl flow at L/D=7. As a general trend, there was no distinct classification but the temperature distribution profile of the swirl flow was lower and simpler than that of the non-swirl.

3.3 The dimensionless temperature

The dimensionless temperature $(T_w-T)/(T_w-T_a)$ is plotted along the distance to the radius as shown in Fig. 16 and Fig. 17. The dimensionless temperature $(T_w-T)/(T_w-T_a)$ is shown with the variation between top and bottom of the test tube with the non-swirl flow for Re=6×10⁴, in Fig. 16. When $\theta=0°$, 30° the dimensionless temperature increased at the tube center, and then decreased and approached 0.55−0.6 at the wall. When $\theta=60°$, 90° and 120°, it increased to half of the radius, and then decreased and increased, approaching the wall. When $\theta=150°$ and 180°, it slightly increased and was constantly maintained at 0.5. It seems that the temperature profiles were affected by the flow pattern from the effects of the tube bend shown in Fig. 17. The dimensionless temperature $(T_w-T)/(T_w-T_a)$ is shown with the variation between the top and bottom of the tube for the swirl flow of L/D=0 at Re=60,000 in Fig. 17. In this case, each section of the tube has a similar temperature profile. The dimensionless temperatures are increased from 0.38 to 0.45 for the range $(y-r)/r=0$ to -0.3, and then decreased.

The swirl flow has small numbers in the dimensionless temperature than in the non-swirl flow and is uniformly distributed compared to non-swirl flow, the swirl flow is less influenced by the profile of the bend tube. The temperatures with swirl can be low and consistently maintained.

3.4 The characteristics of heat transfer

The Nusselt number was calculated from the wall and the bulk temperature of the upstream, bend, and downstream of the test tube and made dimensionless by using the Dittus- Boelter equation for the fully developed flow, and the results are shown in Figs. 18 and 19.

It is similar to the profile, which is suggested by Kays et al.(1980) to be reduced in Nu/Nu_{DB} at the straight tube of the upstream of the bend and at the inner and outer cross-sections of the tube bend entrance. It was shown that the maximum heat transfer occurred at 90° from the non-swirl flow, the Nu/Nu_{DB} increased, maximum at 90° and then decreased. In the swirl flow, the same trend occurred, but the Nu/Nu_{DB} was slightly bigger and less scattered than in the non-swirl flow. It was shown that the swirl flow improves the heat transfer in the 180° bend flow.

The Nusselts number for each Reynolds number of the inner and the outer positions of the bend tube in the non-swirl flow are shown in Fig. 20. It was shown that the Nusselts number of the inner portion of the bend is 2.0 to 2.1 times greater than that at the outer position and maximum at 90° and then decreased.

In case of swirl intensity of L/D=0, the Nusselts number of the bend inner section, the

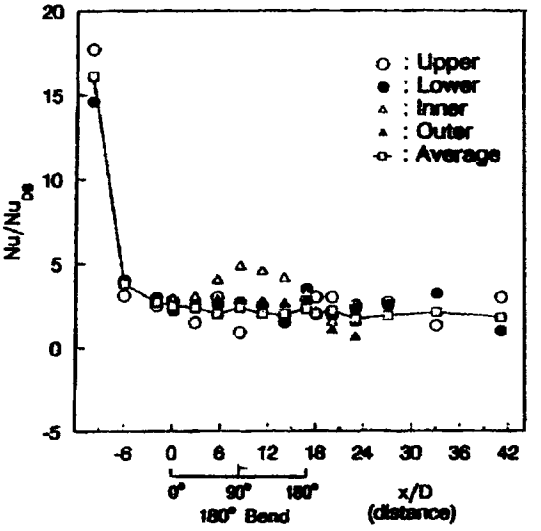

Fig. 19 Profiles of Nu/Nu_{DB} along the test tube with swirl at L/D=7 for Re=6×10^4

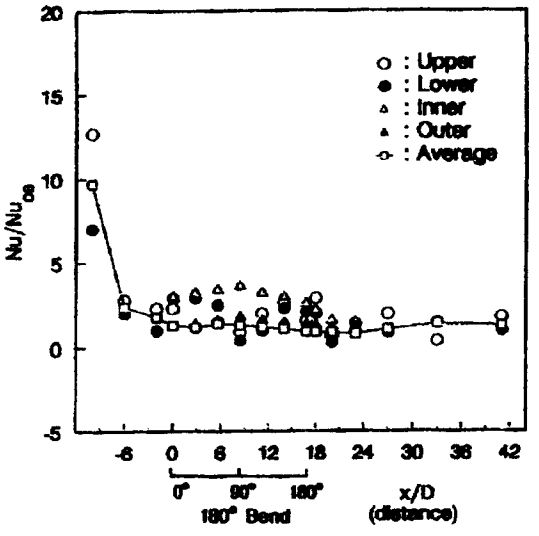

Fig. 18 Profiles of Nu/Nu_{DB} along the test tube with non-swirl for Re=1×10^5

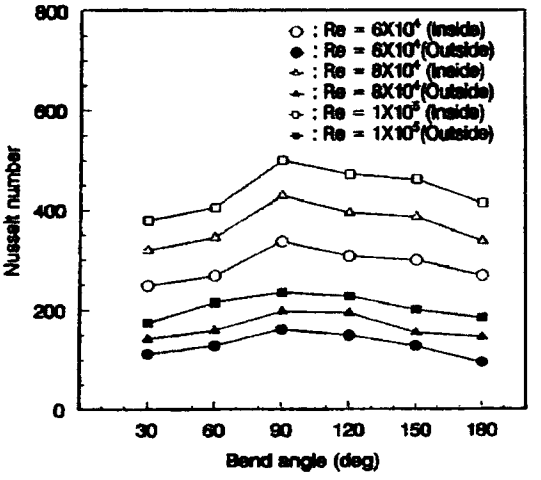

Fig. 20 Comparisons of Nu profiles between the inner and the outer positions along the 180° bend with non-swirl with respect to Re

increment slope, and the overall Nusselts number appeared to be greater than in the non-swirl flow. The Nusselts number of the outer section was shown to be 2.2 to 2.3 times greater than in the outer. This is the results expected based on the investigation of the wall and bulk temperature measurements.

To compare the ratio of the heat transfer coefficient between the swirl flow and the non-swirl flow, the Nusselts numbers and the increased ratios for each flow condition are listed in Table 4. In case of the swirl intensity of L/D=0, the Nusselts number increased 90-100%, compared to the non-swirl flow, and for L/D=7 or L/D=14, there was about a 40-70% increase. As a results in case of the swirl intensity of L/D=0, an intensive swirl flow is operated on the overall test tube, and, in case of L/D=7 or L/D=14, the swirl flow vanishes and changes near the non-swirl flow at the downstream of the test tube.

Where, these data were prepared based on the average temperature and the velocity of the cross-section of the tube, but the effects of the local heat transfer inside the tube was not taken into consideration. The effects of the several flow patterns were considered from cross-section 1 of the upstream to cross-section 16 of the downstream.

Figure 22 is a chart plotted by the Nusselts number, which is converted to be dimensionless for the non-swirl flow of $Re=6\times10^4$ and maximum $Nu/Nu_{DB}=2.5$ at 90° cross-section of the bend. For the swirl flow, maximum Nu/Nu_{DB} is 4.8 at 90° cross-section of the bend. And, as a whole, of the swirl flow is higher than that of the non-swirl. These results are generally consistent with those of Said et al.(1992).

Table 4 Increased ratio of Nusselt number at given flow conditions

Flow condition	Reynolds number	Heat transfer coefficient	Nusselt number [Nu]	Increase Rate [%]
Non-swirl	6×10^4	74	151	–
	8×10^4	88	181	–
	1×10^5	106	218	–
Swirl L/D=0	6×10^4	142	291	93
	8×10^4	176	363	100
	1×10^5	214	440	102
Swirl L/D=7	6×10^4	104	215	42
	8×10^4	146	300	66
	1×10^5	175	360	66
Swirl L/D=14	6×10^4	103	22	40
	8×10^4	139	287	59
	1×10^5	180	371	70

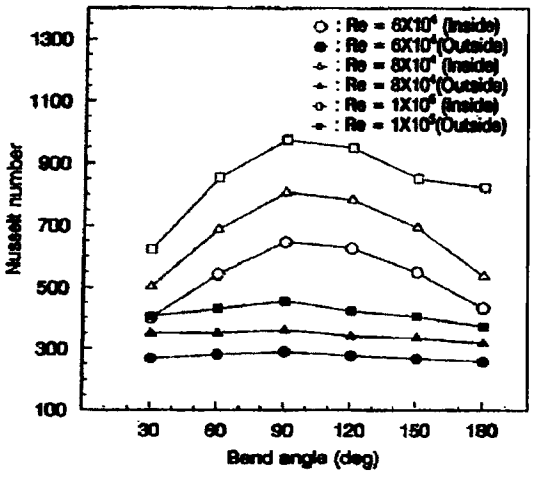

Fig. 21 Comparisons of Nu profiles between the inner and the outer positions along the 180° bend with swirl at L/D=0

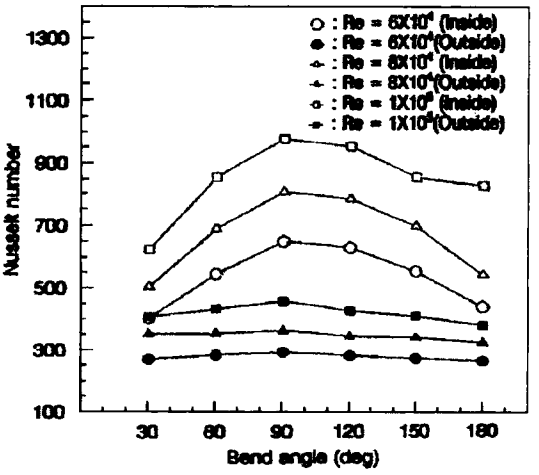

Fig. 22 Comparison of Nusselt number profiles along the 180° bend for $Re=6\times10^4$

This investigation was conducted in case of the fixed ratio between the test tube diameter D and swirl chamber diameter d, but the swirl intensity is to be changed according to the ratio and the entrance conditions. Furthermore, the characteristics of the heat transfer are to be changed, according to change of the curvature ratio.

4. Conclusion

A U-bend circular tube having the curvature ratio of 9.4 was made from a stainless steel tube. The test tube was heated by a voltage regulator and the following conclusions were derived from the experiment of the swirl and non-swirl flow for $Re=6\times10^4$, 8×10^4 and 1×10^5.

(1) Even though the wall temperature continuously increased throughout the length of the tube, the bulk temperature temporarily decreased for the non-swirl flow and reached minimum at $\theta=90°$ and for the swirl flow, the effect of the geometric configuration was lessened and it continuously increased.

(2) The bulk temperature of the non-swirl flow was high and scattered in the same cross section of the tube, scattered but one of the swirl flow was nearly consistent, and continuously increased.

(3) The dimensionless temperature in the swirl flow was kept more consistent and is lower than that in the non-swirl flow.

(4) In the bend tube, the Nusselt number was the maximum at $\theta=90°$ and the Nusselt number at the inner portion of the cross-section of the tube was 2.0 to 2.3 times greater than that of the outer position. The Nusselt number of the swirl flow generally increased, and, in case of the swirl intensity of L/D=0, increased by 90~100%.

(5) When $Re=6\times10^4$, the Nu/Nu_{DB} of the non-swirl flow reached the maximum of 2.5. This profile was very consistent with the results of Said et al.(1992). At the swirl intensity of L/D=7, it was the highest at 4.8.

Acknowledgment

This work is supported by Kyungnam University research fund, 2003.

References

Baughm, J. W., Lacovides, H. Jackson D. C. and Launder, B. E., 1987, "Local Heat Transfer Measurements in Turbulent Flow Around a 180-Deg Pipe Bend," *Journal of Heat Transfer*, Vol. 109, pp. 43~48.

Chang, S. M., Humphrey, J. A. and Modavi A., 1988, "Turbulent Flow in Strongly Curved U-bend and Downstream Tangent of Square Cross Section," *PCH Physico Chemical Hydrodynamic*, Vol. 4, pp. 243~253.

Enayet, M. M., Gibson, M. M., Taylor, A. M., K. P. and Yiannekis, M., 1982, "Laser-Doppler Measurements of Laminar and Turbulent Flow in a Pipe Bend," *Int. J. Heat & Fluid Flow*, Vol. 3, No. 4, pp. 213~220.

Ito, H., 1960, "Pressure Losses in Smooth Pipe Bends," *Journal of Basic Engineering*, pp. 131~139.

Kays, W. M. and Crawford, M. E., 1980, Convective Heat Transfer, Second Edition, McGraw-Hill.

Medwell, J. O., Chang, T. H. and Kwon, S. S., 1989, "A Study of Swirling Flow in a Cylindrical Tube," Korean J. of Air-Conditioning and Refrigeration Engineering, Vol. 1, No. 4, pp. 265~275.

Metha, N. D. and Bell, K. J., 1981, "Laminar Flow Heat Transfer," *Soviet Research*, Vol. 103, No. 6, pp. 71~80.

Mullin, T. and Greated C. A., 1980, "Oscillatory Flow in a Curved Pipe, Part 1 : The Developing Flow Case," J. Fluid Mech. Vol. 98, Part 2, pp. 383~395.

Richard W. Johnson, 1988, "Numerical Simulation of Local Nusselts Number for Turbulent Flow in a Square Duct with a 180 Degree Bend," Numerical Heat Transfer, Vol. 13, pp. 205~228.

Said Dini, Nader Saniei and Daniel Bartlett, 1992, "Use of Liquid Crystal for Local Heat Transfer Coefficient Measurement Around a 180 Degree Bend," ASME, HTD-Vol. 210, pp. 107~114.

Tae-Hyun Chang and Hee-Young Kim, 2001, "A Investigation of Swirling Flow in a Cylin-

drical Tube," *KSME International Journal*, Vol. 15, No. 12, pp. 1892~1899.

Talbot, L. 1954, "Laminar Swirl Flow," J. of Applied Mechanics, ASME, Vol. 21, pp. 1~7.

Thomson, J., 1876, "On the Origin of Winding of River in Alluvial Planic, with Remarks on the Flow of Water Pound Bend in Pipe," duroc. K. Soc. London Ser, A25, pp. 5~8.